Detecting Focal Regions using Superpixels

Richard Lowe and Mark Nixon
CSPC Group, University of Southampton, Burgess Rd, Southampton, U.K.

Keywords: Superpixel, Focus Region, Light Field.

Abstract: We introduce a new method that can automatically determine regions of focus within an image. The focus is determined by generating Content-Driven Superpixels and subsequently exploiting consistency properties of scale-space. These superpixels can be analysed to produce the focal image regions. In our new analysis, Light-Field Photography provides an efficient method to test our algorithm in a controlled manner. An image taken with a light-field camera can be viewed from different perspectives and focal planes, and so by manually modifying the focal plane we can determine if the extracted focal areas are correctly extracted. We show improved results of our new approach compared with some prior techniques and demonstrate the advantages that our new approach can accrue.

1 INTRODUCTION

The ability to focus is implicit in image formation. In photography, there are passive and active approaches to achieve image autofocus wherein the image clarity depends on optical parameters. Passive autofocus approaches analyse local image contrast as part of a feedback mechanism driving the lens motor whereas active approaches aim to sense distance to derive focus capability. As such, we can enjoy clear photographs which can usually be acquired with the object of interest in sharp focus.

In contrast to the plethora of approaches for image autofocus, there are few approaches which can be applied to analyse an image to determine the regions which are in sharp focus. One such approach, the Sum Modified Laplacian (Nayar and Nakagawa, 1994), was designed to analyse shape from focus using the relative differences in contrast at differing image resolutions. More recent works are concerned with the extraction of edge information (Tai and Brown, 2009) as the edges contain more high frequency information. Another method uses Gabor wavelets (Chen and Bovik, 2009) that are tuned to detect high frequency image components. Other methods (Liu et al., 2008; Kovacs and Sziranyi, 2007; Levin, 2007) attempt to model a blur kernel and use convolution to inverse the blurring process. These algorithms are actually de-blurring algorithms and have a different intention (to remove blurring) but operate in a similar way.

The method we choose to compare with is the Sum Modified Laplacian as it is well-established. We also compare with approaches described in (Levin, 2007) and (Liu et al., 2008), though these methods require the tuning of several parameters. They also rely on feedback from human vision to determine if the result is 'correct'. As these rely on sharpness of edge information, they are also sensitive to noise.

We introduce a new approach that can be applied to explicitly extract focal regions of a single image without choice of parameters. By exploiting the combined properties of the scale-space and superpixels, it is possible to extract uniform regions in scale and therefore determine the most likely regions of image focus.

Superpixels are a way of altering the representation of an image. They replace the grid of equally sized pixels with unequal regions that are unique to each image; aiding the description of image objects. As superpixels have the property of shape, they can convey local information about the image. Intuitively, this also improves speed of further processing as superpixels significantly reduce the number of pixels. We use Content-Driven Superpixels (Lowe and Nixon, 2011) since, unlike many superpixel algorithms, they are designed to produce an unspecified number of superpixels that are consistent in colour but not size. Using this in conjunction with a scale-space representation yields a set of superpixels that are uniform with respect to colour across multiple scales. The distribution of superpixels through scale can be used to infer where the image has been affected by smoothing and therefore where the image is in focus as illustrated in Figure 1.

Lowe R. and Nixon M..
Detecting Focal Regions using Superpixels.
DOI: 10.5220/0004212102640270
In *Proceedings of the International Conference on Computer Vision Theory and Applications* (VISAPP-2013), pages 264-270
ISBN: 978-989-8565-47-1

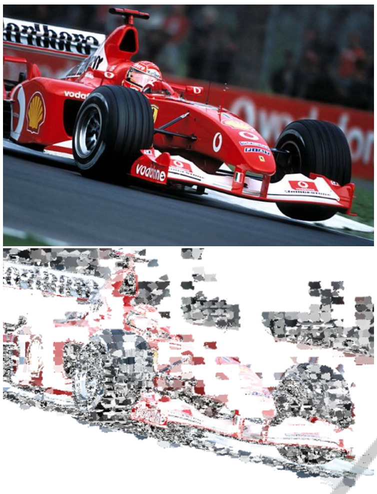

Figure 1: Determining focused areas of an image using superpixels.

With conventional images it is difficult to ascertain, other than with human vision, whether image focus has been correctly localised. For a principled analysis of focus detection, we use Light Field Photography (LFP) to validate our approach as it provides a controlled environment with which to vary the focal plane in an image. Our results can show precisely that as image focus varies, the extracted focus regions of the image correspond to that change.

The paper is arranged as follows: firstly, scale-space is introduced. Content-Driven Superpixels are then described and extended into 3D in order to analyse scale-space. Subsequently, Light Field Photography is described as the method with which to generate the test images to analyse performance. The mechanism of focus detection is then described, followed by a presentation and discussion of the results.

2 SCALE-SPACE

Developed by Witkin (Witkin, 1983), scale-space is a one-parameter family of derived images that successively smoothes an image, removing more high-frequency features with each scale. Among other things, it has been used in detecting scale-invariant edges (Bergholm, 1987), as a basis for the popular SIFT and SURF operators, and also saliency (Kadir and Brady, 2001). Edges are deemed to be more significant if they persist for several scales whereas saliency is more significant if it persists over few scales. To generate the scale-space, the new images need to be derived by convolving the image with a Gaussian filter, given in Equation 1, where t denotes the scale.

$$g(x,y,t) = \frac{1}{\sqrt{2\pi t}} e^{(-\frac{x^2+y^2}{2t})} \tag{1}$$

The choice of t is based on a logarithmic sampling. To efficiently construct the scale-space, t is chosen such that the difference between scales is maximised without losing detail. Equation 2 provides a method of selecting t (Lindeberg, 1994). τ is the transformation of the image as a function of the smoothing parameter t and A is a free parameter. This motives the choice of sampling to be $t = \{1,4,16,64,256\}$, the use of which causes the logarithmic sampling to produce a linear increase in value for A and therefore a linear difference between scales.

$$\tau(t) = A \log t \tag{2}$$

The scale-space is then collapsed into a single volume, successive two-dimensional slices represent increasing levels of detail.

We can infer from the scale-space that if a spatial region is consistent over all scales then smoothing has had little effect. Therefore this region contains little high frequency information and is more likely to be out of focus.

3 CONTENT-DRIVEN SUPERPIXELS

Content-Driven Superpixels (CDS) (Lowe and Nixon, 2011) is a new approach designed to allow superpixel coverage to express the underlying structure of an image. An image will contain as many superpixels as needed and is not controlled by initialisation parameters. As such, it is an appropriate way of exploring how the scale-space changes with increased smoothing, without imposing supervised initialisation.

The CDS approach is designed to grow superpixel regions, splitting them as they become more complex in order to retain colour uniformity. Extending this to consider the scale-space means that the superpixels will represent uniform colour in scale and in space. The distribution will describe the underlying structure of the scale-space and this information can be analysed to determine the focal regions. These superpixels shall be referred to as supervoxels as they occupy a third dimension, despite the fact that this third dimension is not spatial.

3.1 Extending the Algorithm to 3D

Fortunately, as CDS is a combination of standard spatial computer vision techniques, each sub-process can be separately transposed into 3D. The two main mechanisms: 'Distance Transform' and 'Active Contours without Edges' are ideally suited for 3D.

3.1.1 Distance Transform

Supervoxel growth is achieved using a distance transform of every supervoxel. This transforms each supervoxel S such that a set of voxels at locations i, j, k within the supervoxel display the distance D to the background (in this case, the region in which supervoxels have yet to form). Supervoxel edges therefore have a distance of one from the background. A binary volume V is used to calculate the distance transform where *True* denotes that a supervoxel covers this point in the volume and *False* otherwise. The background is therefore all the *False* points. The same volume is used to individually grow each supervoxel.

The Distance Transform in 3D transforms a volume such that the volume displays the distance D of each voxel at location $(i, j, k)$to the nearest background location (x, y, z). This is given in Equation 3.

$$D = \min_{x,y,z:\ V(x,y,z)=False} \sqrt{(i-x)^2+(j-y)^2+(k-z)^2} \tag{3}$$

This growth occurs at each iteration t. The growth of the supervoxel S is given in Equation 4.

$$S^{<t+1>} = S^{<t>} \cup \{(x,y,z)\colon D(x,y,z) = 1\} \tag{4}$$

3.1.2 Active Contours without Edges

Active Contours Without Edges (ACWE) (Chan and Vese, 2001; Chan et al., 2000) aims to partition an image into two regions of constant intensities of distinct values. These values form the positive and negative parts of a signed distance function, Ω_D . Equation 5 describes the force F that iteratively updates the distance function. For example F is large and negative for a particular pixel if it is currently labelled as positive and is distinct from the mean of the region that it is contained in. F is small for a pixel if it is similar to the mean of the region it is contained in. By iteratively updating the distance function of each pixel, the boundary between the positive and negative regions moves. Each voxel therefore becomes part of the region it best matches.

The new supervoxels, C_u, C_v , are taken to be the positive and negative parts of the newly formed distance function, Ω'_D. To use this algorithm with supervoxels it is necessary to define $\Omega(x,y,z)$ as a vector that contains a set of all the voxels within the supervoxel.

$$\begin{aligned} F(x,y,z) = & \int_\Omega \frac{1}{N}\sum_{i=1}^{N} |I_i(x,y,z) - u_i|^2 dxdydz \\ & - \int_\Omega \frac{1}{N}\sum_{i=1}^{N} |I_i(x,y,z) - v_i|^2 dxdydz \end{aligned} \tag{5}$$

The segmentation criterion of either region u, v is given as the average of the means (u_i, v_i) of each of the N colour channels V_i of the volume V; shown in Equation 6. Supervoxel division occurs if there is a significant difference between any of the colour channels.

$$\begin{aligned} u_i &= \frac{\int_\Omega V_i(x,y,z)dxdydz}{\int_\Omega \Omega(x,y,z)dxdydz}, \forall \Omega_D(x,y,z) > 0 \quad (6) \\ v_i &= \frac{\int_\Omega V_i(x,y,z)dxdydz}{\int_\Omega \Omega(x,y,z)dxdydz}, \forall \Omega_D(x,y,z) \leq 0 \end{aligned}$$

ACWE still requires the separation of a supervoxel into two regions u, v, but these regions now occupy a 3D signed distance function $\Omega_D(x,y,z)$. The two regions C_u, C_v are given in Equation 7.

$$\begin{aligned} C_u &= \{(x,y,z) : \Omega'_D(x,y,z) > 0\} \quad (7) \\ C_v &= \{(x,y,z) : \Omega'_D(x,y,z) \leq 0\} \end{aligned}$$

3.2 Applying CDS to Focus Detection

Firstly, images are converted into a set of 3D scale-space representations using the values of t defined in Section 2. By using scale-space for superpixels, the aim is to produce superpixels that have context over scale; scale-persistent superpixels are more likely to be stable whereas scale-varying superpixels are more likely to be in feature-rich areas of the image.

By grouping regions of scale-space, it is possible to gain information about the nature of that region of the image. The idea is that superpixels that exist in the low detail area of the scale-space are less likely to contribute the high-frequency content present in the focused region of the original volume. A set of supervoxels is initialised in the least-detailed layer of the scale-space. This is done such that as the supervoxels grow through more complex layers of the space, they increase in number. Initialising in the most complex layer would require more supervoxels than necessary to represent the least complex layer.

To reveal the parts of the image, as the volume being analysed is smoothed, the most smoothed layer will contain the least information. The focus is determined as the lowest detail layer t_{min} in which the supervoxel still exists. Therefore the supervoxels that exist in the first layer have the lowest focus value. Supervoxels that exist solely in the highest layer have

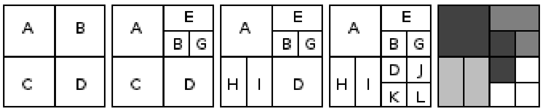

(a) $t = 0$ (b) $t = 1$ (c) $t = 2$ (d) $t = 3$ (e) *Result*

Figure 2: Illustrating how focus is determined.

the maximum focus value. This is shown in Equation 8. The focus measure F for a supervoxel s is controlled by the first layer t in which that supervoxel exists. $T_{\max}$ is the number of layers in the image.

$$F(s) = \frac{1}{T_{\max} - min\{t : s(x,y,t) > 0\}}; (x,y) \in I, 0 \leq t < T_{\max} \quad (8)$$

A hypothetical example is given in Figure 2, which shows four layers of the same volume, where each labelled region represents a supervoxel. Multiple layers can contain the same supervoxel, for example region A which exists for all layers, but the minimum layer is $t = 0$. Each subfigure is given with the layer t in the volume it represents. Figure 2(d) shows the least smoothed layer, ie. the original image.

As region A remains constant, no change in space or scale has been detected and can be considered out of focus. Regions A,B,C,D are therefore given a focus value of $F(s) = 0.25$. Next E,G have a focus of 0.5 as they first exist in layer $t = 1$, and regions H,I have a focus value of 0.75. Regions J,K,L are therefore the most likely to be in focus, with $F(s) = 1$. Figure 2(e) shows this graphically, where brightness indicates a higher focus value. Each location in space shows the highest focus value at that point. For example in the case of regions C,H,I, even though they occupy the same spatial location, the focus values of H and I are given as the result as they have the higher focus value.

4 SUM MODIFIED LAPLACIAN

As a comparative approach, an established method of analysing focus is the Sum Modified Laplacian (SML). The focus is derived from the image I at levels spaced by a step Δs.

$$\begin{aligned} \text{ML}(x,y) = &|2I(x,y) - I(x-\Delta s, y) - I(x+\Delta s, y)| \\ &+ |2I(x,y) - I(x, y-\Delta s) - I(x, y+\Delta s)| \quad (9) \end{aligned}$$

The focus measure (Equation 10) at (i,j) is evaluated as the neighbourhood (of size N) sum of the modified Laplacian (Equation 9) which exceed a threshold T. The step size can be varied to locate different texture sizes.

$$F(i,j) = \sum_{x=i-N}^{i+N} \sum_{y=j-N}^{j+N} \text{ML}(x,y) | \text{ML}(x,y) \geq T \quad (10)$$

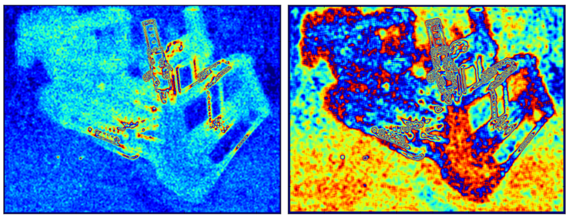

(a) $N = 2$ (b) $N = 4$

Figure 3: Showing the same image using different values for N in SML. The red areas depict distinctly different areas of focus in each image.

This is problematic as it will only select textures of a chosen size and will be affected by the size of the neighbourhood. This makes using the algorithm as a focus measure subject to human opinion and insight. The results of focus detection in Figure 3 show that the quality of the result relies on selection of appropriate parameter values, and the selection of those parameters relies on human visual analysis. This property is not a problem if one is comparing images generated using the same parameters.

In contrast, our new approach can inherently locate scale-varying regions without parameterisation or supervision. CDS also is region based, thereby selecting regions of interest which is more useful than individual pixels.

5 GENERATING THE TEST IMAGES

Light Field Photography (LFP)(Levoy and Hanrahan, 1996) is continuing to gather interest. LFP is currently achieved (Wilburn et al., 2005) using either an array of cameras or a single camera moved through a 2D array. A capture method using a single exposure (Ng et al., 2005; Adelson and Wang, 1992) is now being developed commercially. By considering an image as a 2D slice of a 4D function, new views of the same scene can be obtained by extracting different slices. This is exploited in several ways, the relevant one in this case being the ability to refocus a light-field after it has been taken.

We use this ability is used to generate controlled test images. This allows a principled analysis of focus, this being the first time such a test procedure has been achieved. A series of images are chosen from a light-field that focus on a different section of the scene, thereby allowing the efficacy of focus detection to be measured. An example series of images is given in Figure 4 which shows ability of LFP to focus on foreground and background objects.

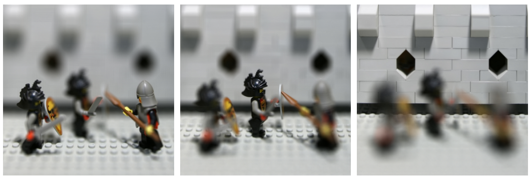

(a) near (b) middle (c) far

Figure 4: Illustrating the effect of change of focus on a light-field.

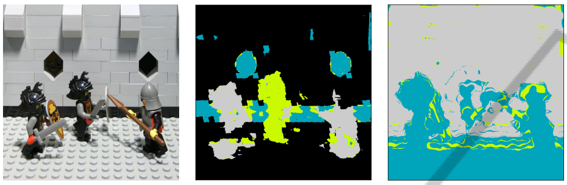

(a) Reference image (b) The labelled focus response of each image (c) The labelled SML response of each image

Figure 5: Result on the lego image.

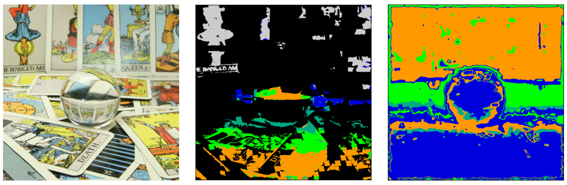

(a) Reference image (b) The labelled focus response of each image (c) The labelled SML response of each image

Figure 6: Result on the image containing tarot cards.

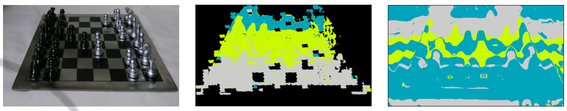

(a) Reference image (b) The labelled focus response of each image (c) The labelled SML response of each image

Figure 7: Result for the chess image.

6 RESULTS

6.1 Light-field Experiments

We evaluate our algorithm using the controlled images derived from light fields. There are two ways of analysing the quality of the results. Firstly, the ‘focus response’, where the supervoxels are drawn on the image as an alpha layer to show which parts are in focus. This response is then used in conjunction with the depth information of the light field to determine which depths of the image are extracted as ‘in focus’. This can then be used to label the image with the corresponding depths. The images in this section are taken from light-field images available through the Stanford Computer Graphics Laboratory [1]. All SML images are generated using $T = 1$ and $\Delta S = 1$ which retains the highest proportion of high-frequency information.

Figure 5 shows the result on the lego image in Figure 4. Figure 5(a) shows the image totally in focus for reference. Figure 5(b) shows the focus of each image as the focal depth changes. The coloured labels correspond to the focus of different images, and so here the change in focus through the image can be observed by areas of the image being occupied by distinct bands of colour. Grey corresponds to image 0, green to image 1 and blue to image 2. Black regions were not labelled as in focus in any image. CDS clearly shows the change in focus in the image, whereas SML incorrectly misses the central figure and mis-labels the background.

Figure 6 shows the response to a light-field image containing tarot cards. The CDS response is shown in Figure 6(b) where the objects at each depth belong to different image labels when the object was in focus. Orange corresponds to image 0; green to image 1; cyan to image 2; blue to image 3 and grey to image 4. Here, the SML response shows no clear distinction between the images, and the bands present in the CDS response are missing. There is also significantly more noise, as most of the pixels are labelled as being in focus, whereas CDS shows clear regions of no focus at all.

The image in Figure 7 again shows a clear transition from foreground to background as the focus of the image changes. In the CDS response there is once again a clear separation of each response, SML cannot correctly distinguish the focus as the focal depth changes. CDS can determine which parts of the image is background whereas SML cannot.

6.2 Image Experiments

Figure 8 compares the result from CDS with three other techniques. The brightness of the result denotes how focused that area is. It is difficult to compare with other approaches as only the classification result is available and their techniques are not yet evaluated using LFP. However, we detect largely the same regions as both. There is some inclusion of the background, however this is at a lower focus value to the cyclist. The CDS approach requires no tuning which is implicit in all other techniques. CDS clearly detects the focused cyclist well.

The algorithm has also been applied to several

[1] http://lightfield.stanford.edu/

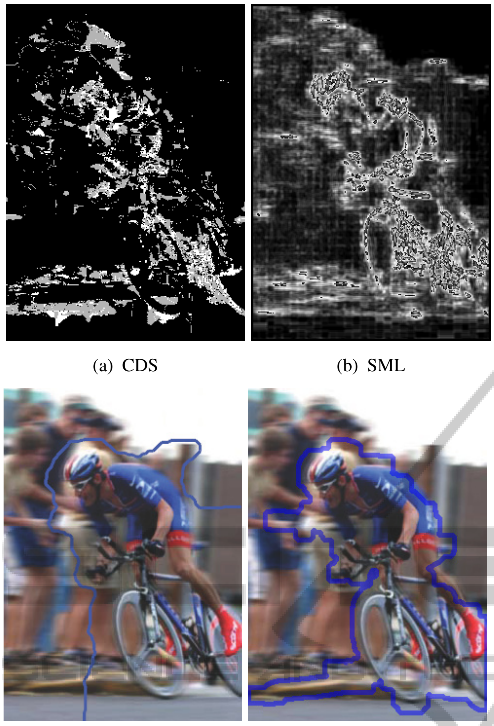

(a) CDS (b) SML

(c) Levin (Levin, 2007) (d) Liu (Liu et al., 2008)

Figure 8: Comparing CDS with other techniques.

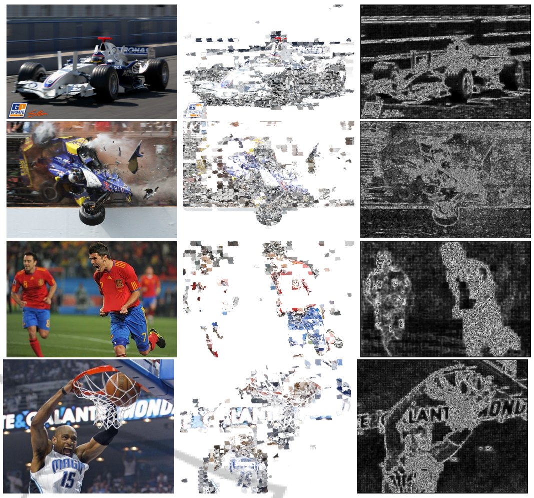

(a) Original (b) CDS (c) SML

Figure 9: Sports images.

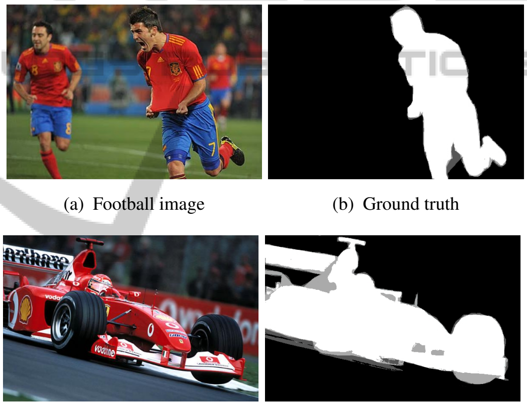

(a) Football image (b) Ground truth

(c) Car image (d) Ground truth

Figure 10: Test images used to compare SML and CDS.

Table 1: Results on two images to show the percentage of the response that corresponds with a ground truth.

Technique	Football	Car
CDS	0.49	0.60
SML Min	0.21	0.40
SML Max	0.43	0.74

sports images shown in Figure 9. Motorsport images are particularly suited to illustrating the ability to extract focused regions since the images produced contain large amounts of motion blur. Note that neither technique extracts regions of uniform colour. This is because, inherently, contrast does not change in uniform regions.

There are notable differences between CDS and SML. Firstly, SML does a much better job of extracting the basketball image. However in the car images, SML detects areas of erroneous focus in the background that are attributed to strong edge information. As CDS does not rely on edge information to detect focus, these regions are not detected in our new approach.

Table 1 compares the two images in Figure 10 for both SML and CDS by calculating the fraction of the output that is contained within the ground truth. The ground truth was derived by averaging the response of five different human 'labelers'. The 'labelers' were instructed to highlight the regions of the image which appeared to be in sharp focus. This implies that some uniform areas are manually labelled to be in sharp focus whereas these areas are detected by neither SML nor CDS. It shows that while SML can sometimes have a better response, it is highly dependent on the input parameters to the algorithm; the results can vary by as much as 50%. CDS performs as well as the best SML result without supervision or manual intervention. An analysis by human 'labelers' also introduces some confusion as in the football image one player is not labelled however it is detected by both algorithms as shown in Figure 9.

7 DISCUSSION

Any image can contain both focused and unfocused regions. There is no way to test the validity of a focus detection algorithm without a reliable metric which can quantify focus accuracy. By using the depth information from the light field we have shown that it is possible to show that the focal response corresponds to a specific image depth and that this depth changes consistently with image focus.

Essentially, CDS highlights the parts of the image that are in focus but also are more likely to contain high-frequency information. As CDS creates new superpixels on detecting image variation, there will be some constant colour areas of the image that do not change significantly with blurring. The result will be that these regions are not marked as in focus. While other methods can extract points of focus within the image, these methods rely on tuning of the algorithm parameters. As we have shown, the results on SML can vary by as much as 50% depending on the selection of adequate parameters. In addition, as these are edge based techniques, they also rely on the absence of noisy edges in the image. CDS negates this by considering regions within the image, as there is an inherent averaging within ACWE.

This paper has described the first application of superpixels in conjunction with scale-space. Applying CDS to the task of focus detection gives a result which has been shown to correspond accurately to the focal regions of the image. Crucially, it is unsupervised and as such gives an unbiased representation of the focus within an image, which can be demonstrated by using the unique properties of Light Field Photography.

REFERENCES

Adelson, E. H. and Wang, J. Y. A. (1992). Single lens stereo with a plenoptic camera. *IEEE Transactions on Pattern Analysis and Machine Intelligence*, 14(2):99–106.

Bergholm, F. (1987). Edge Focusing. *IEEE TPAMI*, 9(6):726–741.

Chan, T., Sandberg, B., and Vese, L. (2000). Active Contours without Edges for Vector-Valued Images. *Visual Communication and Image Representation*, 11(2):130.

Chan, T. F. and Vese, L. A. (2001). Active Contours Without Edges. *IEEE Trans. Image Processing*, 10(2).

Chen, M.-J. and Bovik, A. C. (2009). No-reference image blur assessment using multiscale gradient. In *Quality of Multimedia Experience, 2009. QoMEx 2009. International Workshop on*, pages 70–74.

Kadir, T. and Brady, M. (2001). Saliency, Scale and Image Description. *IJCV*, 45(2):83–105.

Kovacs, L. and Sziranyi, T. (2007). Focus area extraction by blind deconvolution for defining regions of interest. *Pattern Analysis and Machine Intelligence, IEEE Transactions on*, 29(6):1080–1085.

Levin, A. (2007). Blind motion deblurring using image statistics. *Advances in Neural Information Processing Systems*, 19:841.

Levoy, M. and Hanrahan, P. (1996). Light field rendering. In *Proc. Conf. on Computer Graphics and Interactive Techniques*, pages 31–42.

Lindeberg, T. (1994). Scale-space theory: A basic tool for analyzing structures at different scales. *Journal of Applied Statistics*, 21(1):225–270.

Liu, R., Li, Z., and Jia, J. (2008). Image partial blur detection and classification. In *Computer Vision and Pattern Recognition, 2008. CVPR 2008. IEEE Conference on*, pages 1–8.

Lowe, R. and Nixon, M. (2011). Evolving Content-Driven Superpixels for Accurate Image Representation. In *Proc. ISVC2011*, volume 6938 of *Lecture Notes in Computer Science*, pages 192–201. Springer-Verlag.

Nayar, S. K. and Nakagawa, Y. (1994). Shape from focus. *Pattern Analysis and Machine Intelligence, IEEE Transactions on*, 16(8):824–831.

Ng, R., Levoy, M., Brédif, M., Duval, G., Horowitz, M., and Hanrahan, P. (2005). Light field photography with a hand-held plenoptic camera. *Computer Science Technical Report CSTR*, 2.

Tai, Y.-W. and Brown, M. S. (2009). Single image defocus map estimation using local contrast prior. In *Image Processing (ICIP), 2009 16th IEEE International Conference on*, pages 1797–1800.

Wilburn, B., Joshi, N., Vaish, V., Talvala, E. V., Antunez, E., Barth, A., Adams, A., Horowitz, M., and Levoy, M. (2005). High performance imaging using large camera arrays. *ACM Transactions on Graphics*, 24(3):765–776.

Witkin, A. (1983). Scale-space filtering. *Intl. Joint Conf. Art. Intell.*, 2:1019–1022.